Los Alamos NATIONAL LABORATORY EST.1943

LA-UR-18-26917 (Accepted Manuscript)

Simulating Surface and Subsurface Water Balance Changes Due to Burn Severity

Atchley, Adam Lee
Kinoshita, Alicia
Lopez, Sonya
Trader, Laura
Middleton, Richard Stephen

Provided by the author(s) and the Los Alamos National Laboratory (2019-07-17).

To be published in: Vadose Zone Journal

DOI to publisher's version: 10.2136/vzj2018.05.0099

Permalink to record: http://permalink.lanl.gov/object/view?what=info:lanl-repo/lareport/LA-UR-18-26917

Disclaimer:
Los Alamos National Laboratory, an affirmative action/equal opportunity employer, is operated by Triad National Security, LLC for the National Nuclear Security Administration of U.S. Department of Energy under contract 89233218CNA000001. By approving this article, the publisher recognizes that the U.S. Government retains nonexclusive, royalty-free license to publish or reproduce the published form of this contribution, or to allow others to do so, for U.S. Government purposes. Los Alamos National Laboratory requests that the publisher identify this article as work performed under the auspices of the U.S. Department of Energy. Los Alamos National Laboratory strongly supports academic freedom and a researcher's right to publish; as an institution, however, the Laboratory does not endorse the viewpoint of a publication or guarantee its technical correctness.

RESEARCH LIBRARY

Published October 4, 2018

Original Research

Core Ideas

- Burn severity data informed a hydrologic model to assess water balance changes.
- Loss of vegetation and evapotranspiration exceeded impact of increased runoff.
- High burn severity may cause drier site conditions due to increased runoff.
- Change in evapotranspiration acts at long timescales while runoff is event based.

Simulating Surface and Subsurface Water Balance Changes Due to Burn Severity

Adam L. Atchley,* Alicia M. Kinoshita, Sonya R. Lopez, Laura Trader, and Richard Middleton

Forest fires have a significant impact on hydrology, such as reduced infiltration rates leading to increased flooding. However, post-fire water balance changes and the competing hydrologic response of increased runoff and evapotranspiration as a function of burn severity are not well understood. Comparing pre- and post-fire water balance changes is challenging because measurements of fire-disturbed landscapes with the previously undisturbed character are impractical due to non-repetitive observational conditions. We used a physically based modeling experiment to incorporate burn severity data from the Las Conchas fire to approximate model parameterization to evaluate continuous water balance progression for pre- and post-fire simulations using the same forcing conditions. Fire disturbance decreased evapotranspiration and increased overland flow response to precipitation events. The reduction of evapotranspiration often dominated the new water balance compared with the increase in overland flow, resulting in higher soil moisture. However, this modeling experiment also identified a tipping point where increased overland flow from high burn severity sites eclipses the effect of reduced evapotranspiration on the water balance, causing comparatively drier post-fire soils. In particular, high burn severity sites approach a threshold that results in larger changes to overland flow than changes in evapotranspiration, potentially moving the site to an overland flow dominated regime. The shifts in water balance components have implications for how site conditions will change under a range of burn severity scenarios.

Abbreviations: CLM, Community Land Model; DBH, diameter at breast height; dNBR, differenced Normalized Burn Ratio; ET, evapotranspiration; LAI, leaf area index.

A.L. Atchley and R. Middleton, Los Alamos National Lab., Los Alamos, 87545 NM; A.M. Kinoshita, Dep. of Civil, Construction, and Environmental Engineering, San Diego State Univ., San Diego, 92182 CA; S.R. Lopez, Dep. of Civil Engineering, California State Univ., Los Angeles, 90032 CA; L. Trader, Bandelier National Monument, Los Alamos, NM 87544. *Corresponding author (aatchley@lanl.gov).

Received 6 May 2018.
Accepted 18 July 2018.
Supplemental material online.

Citation: Atchley, A.L., A.M. Kinoshita, S.R. Lopez, L. Trader, and R. Middleton. 2018. Simulating surface and subsurface water balance changes due to burn severity. Vadose Zone J. 17:180099. doi:10.2136/vzj2018.05.0099

© Soil Science Society of America.
This is an open access article distributed under the CC BY-NC-ND license (http://creativecommons.org/licenses/by-nc-nd/4.0/).

Forest fire disturbances are becoming increasingly common worldwide due to fire suppression efforts and climate change (Littell et al., 2016; Pechony and Shindell, 2010; Westerling et al., 2006; Wotton et al., 2010), and many of these are developing into a new class of wildfire termed "mega-fires" (Bladon et al., 2014). Mega-fires, such as the 2011 Las Conchas Fire in New Mexico, create large mosaics of disturbed landscapes with varying degrees of burn severity. Fire disturbance in general, and especially mega-fires, can have drastic impacts on the hydrologic response of affected watersheds (Cannon, 2001; Cannon and Reneau, 2000). Moreover, the consequences of wildfire are increasing and often pose risks to society (Kinoshita et al., 2016), particularly post-fire erosion, water supply impacts, and destructive flash flooding as occurred at the Bandelier Visitor Center in 2011 and 2013 following the Las Conchas Fire. This demonstrates a critical need to integrate hydrologic processes into water supply risk assessments (Martin, 2016), which requires detailed understanding of fire effects on the coupled surface and groundwater components of the hydrological cycle.

Fire disturbance alters ecosystems by reducing vegetation and groundcover such as litter and duff (Keeley, 2009). This disrupts the contributions of each component of the water balance, where major changes occur primarily between overland flow and evapotranspiration (ET) (Poon and Kinoshita, 2018). Burn severity, a metric of above- and belowground organic matter loss (Keeley, 2009), is linked to decreased hydrologic conductivity (Moody et al., 2016) and increased surface runoff above a minimum rainfall intensity (Moody et al., 2008). The absence of litter and duff in experimental and observed burned

plots contributes to infiltration-excess overland flow (Cawson et al., 2013; Stoof et al., 2015). The removal of this highly porous layer and the loss of surface soil protection by organic matter causes pore sealing from rain splash and ash particulates (Larsen et al., 2009; Woods and Balfour, 2010), resulting in reduced infiltration rates. Additionally, intense heat fluxes into the soil can cause hydrophobicity and hyper-dry conditions, further decreasing infiltration rates (e.g., DeBano, 2000; Moody and Ebel, 2012). The rapid runoff response to precipitation events due to fire-induced changes in vegetation and soils (e.g., Cawson et al., 2012; Ice et al., 2004; Moody and Ebel, 2014; Moody et al., 2008, 2013) could potentially decrease soil moisture and local groundwater recharge.

Observational studies have documented that fire disturbance leads to an increase in soil moisture compared with unburned sites (Cardenas and Kanarek, 2014; Ebel et al., 2015). This is in contrast to known processes such as increased overland flow that would conceivably lead to decreased soil moisture. However, the increase in soil water recharge is attributed to decreased interception and transpiration (Silva et al., 2006; Soto and Diaz-Fierros, 1997). Both transpiration and interception are functions of vegetation densities, specifically canopy foliage content—often measured as leaf area index (LAI) (e.g., Asner et al., 2003; Bréda and Granier, 1996; Vertessy et al., 1995)—and changes in LAI can be a proxy for burn severities (Boer et al., 2008). Increases in base flow following fire (Wine and Cadol, 2016; Kinoshita and Hogue, 2011, 2015) further suggest increased catchment water storage, probably resulting from elevated soil moisture and groundwater recharge despite water losses due to episodic infiltration-excess overland flow events. Therefore, hillslopes that experience fire disturbance may produce more overland flow, decreasing the local water balance, or conversely retain water due to reduced interception and ET. However, quantification of the change in pre- to post-fire water balance and partitioning among hydrologic processes due to burn severity is rare.

Determining both infiltration-excess overland flow and soil moisture changes as a result of wildfire disturbances requires a coupled understanding of surface and subsurface hydrological processes. Saturation and infiltration-excess overland flow are affected by antecedent soil moisture (Merz and Plate, 1997; Kampf, 2011). Likewise, ET fluxes from the surface and subsurface are influenced by infiltration rates that contribute to energy-limited vs. water-limited latent heat fluxes (Atchley and Maxwell, 2011). Limited studies (Bellot et al., 2001; Ebel, 2013) have discussed the altered interplay between overland flow and soil moisture or groundwater conditions following fire disturbance and have argued for an integrated surface and subsurface hydrologic representation to improve water budget assessments following fire disturbance.

Quantifying the impacts of overland flow and ET on water balances in fire-disturbed landscapes is challenging because pre- and post-fire hydrologic measurements are often unavailable due to the unpredictable nature of wildfires and economic feasibility for long-term monitoring (Kinoshita et al., 2016; Tetzlaff et al., 2017). Furthermore, replicating consistent meteorological hillslope conditions between burned and unburned areas to provide a consistent comparison is impractical. Thus, simulation-based studies that are a simplification of nature but also control for all the unknown variables that may affect the hydrologic outcome are needed to isolate impacts to surface and subsurface hydrologic processes after fire (Ebel, 2013). Furthermore, by simulating transient behavior, these models can evaluate the gradual or episodic nature of hydrologic processes. Using physically based models that control all variables within a domain to simulate pre- and post-fire conditions and explore the impacts of burn severity on the water balance would provide a measured understanding of the interacting hydrological processes after fire disturbances.

The primary objective of this work was to investigate the interplay between overland flow and ET for several burn severity scenarios to quantify possible water balance responses at the hillslope scale. We utilized a coupled surface and subsurface numerical model to isolate the effects of burn severity on overland flow, ET, and soil moisture for the same forcing conditions. To achieve this objective, we (i) parameterized and simulated the hillslope surface and subsurface hydrology using pre- and post-fire vegetation and burn severity data; (ii) estimated the impacts of burn severity on the hillslope water balance; and (iii) identified how and when infiltration-excess surface runoff or ET dominate the hillslope water balance.

Methods

The hydrological model ParFlow-CLM (Version 895) (Ashby and Falgout, 1996; Maxwell, 2013), used to simulate pre- and post-fire disturbance hydrology, is a fully coupled, surface–subsurface, distributed hydrological model. Parameterization of this model allowed us to investigate the water balance response due to LAI, litter-duff depth, and near-surface hydraulic conductivity subjected to varying degrees of burn severity. A 50- by 50-m domain with 2-m horizontal discretization was created to represent 2500-m^2 hillslopes (Fig. 1) for six monitoring sites in the upper Frijoles Canyon of Bandelier National Monument, New Mexico. The near-surface soil was resolved to 1-cm vertical discretization to capture fine-scale infiltration and overland flow processes as a result of litter-duff depth changes and surface soil characteristics. The remaining subsurface layers were gradually increased to an 18-cm discretization by increasing the grid cell depth every four cells below the first eight surface soil cells to the estimated depth of bedrock at 2 m (Soil Survey Staff, 2015).

Measured vegetation characteristics were used to estimate pre- and post-fire LAI. Measured litter-duff layer depth was incorporated in the model mesh, with corresponding organic layer hydrologic properties. The relation between the differenced Normalized Burn Ratio (dNBR) (Key and Benson, 2006) and altered saturated hydraulic conductivity described by Moody et al. (2016) provided estimates of near-surface hydraulic conductivity reduction, a critical consequence of fire on infiltration rates (e.g.,

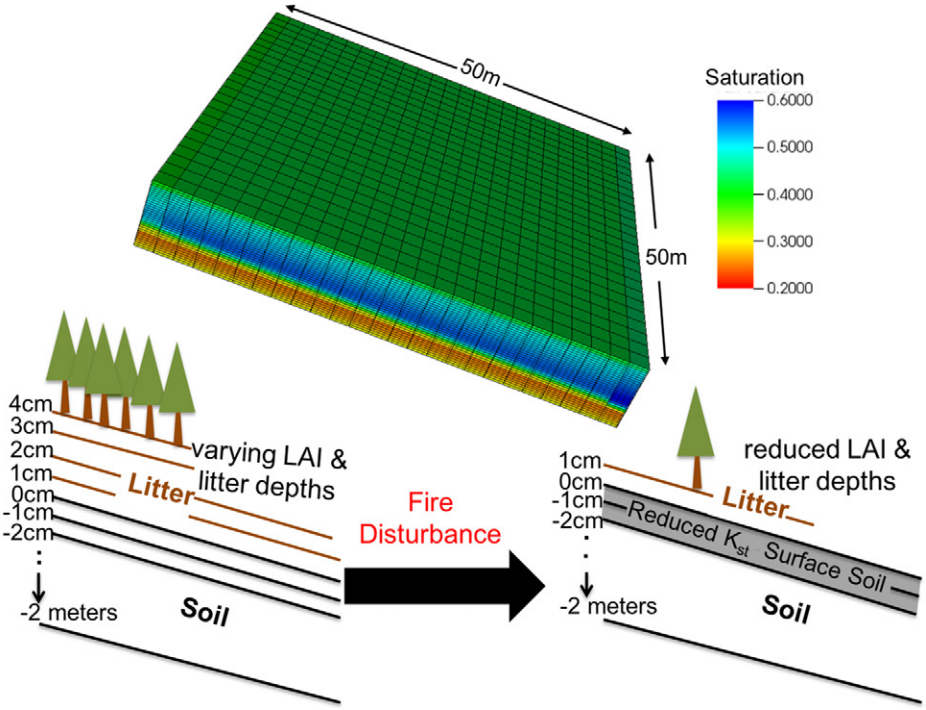

Fig. 1. Simulated soil saturation on 19 July 2013 (top), and a conceptual diagram showing the pre- and post-fire variable leaf area index (LAI), litter-duff depths (0–4 cm), and surface affected soils (bottom).

Moody et al., 2013). The pre- and post-fire domains used the 2013 and 2014 summer convective storm seasons to isolate the effects of burn severity on water balance changes.

Model Description

ParFlow is a surface and variably saturated three-dimensional subsurface flow model (Ashby and Falgout, 1996; Jones and Woodward, 2001; Kollet and Maxwell, 2006) that is coupled with a modified version of the Community Land Model (CLM) (Dai et al., 2003; Ferguson et al., 2016; Jefferson and Maxwell, 2015; Kollet and Maxwell, 2008; Maxwell and Miller, 2005; Mikkelson et al., 2013). The CLM solves ET components using a surface energy balance formulation. Overland flow and groundwater–surface water are coupled by solving the three-dimensional Richards equation, as described in the Supplemental Material SI.1. The CLM coupling provides the source–sink term q_s in the Richards equation and q_r in the kinematic wave equation as precipitation or canopy throughfall inputs and ET sinks. The CLM energy balance formulation used for ParFlow was described in detail by Maxwell and Miller (2005), Jefferson and Maxwell (2015), Jefferson et al. (2017), and in the Supplemental Material SI.2. Land surface energy budget parameters for CLM, including land and plant surface albedo and atmospheric mixing, were provided by Breuer et al. (2003) and the International Geosphere–Biosphere Programme evergreen needleleaf forest land cover values, which did not change between pre- and post-fire simulations, with the exception of LAI. The LAI governs transpiration (Eq. [6] and [7] in Supplemental Material SI.2), throughfall, canopy storage (Eq. [9] and [10] in Supplemental Material SI.2), and soil surface shading was specified for each site as estimated from pre- and post-fire field measurements.

Site Description

Six mixed conifer sites on approximately 20% slopes with varying burn severities from the Las Conchas Fire were chosen in the upper Frijoles Canyon of Bandelier National Monument (Fig. 2) to parameterize the numerical experiment. The six study sites range between 2666 and 2720 m elevation on volcanically derived soils with a mixed conifer vegetation community consisting of ponderosa pine (*Pinus ponderosa* Lawson & C. Lawson), Douglas-fir [*Pseudotsuga menziesii* (Mirb.) Franco], white fir [*Abies concolor* (Gord. & Glend.) Lindl. ex Hildebr.], aspen (*Populus tremuloides* Michx.), limber pine (*Pinus flexilis* James), and Engelmann spruce (*Picea engelmanii* Parry ex Engelm.). The Las Conchas Fire burned approximately 63,400 ha from 26 June to 3 Aug. 2011 (Dahm et al., 2015). The dNBR for the six sites (Table 1), downloaded from the Rapid Assessment of Vegetation Conditions (RAVG) dataset maintained by the US Forest Service, provided a quantitative assessment of burn severity. Vegetation surveys were used to ground-truth burn severity (see below). The RAVG dataset classified the Las Conchas Fire as 31.1% high severity (dNBR > 640), 5.6% moderate severity (315 < dNBR > 640), 38.7% low severity (dNBR < 315), and 24.6% unburned (dNBR < 70). Pre-fire (2005–2007) and post-fire (2011) photos of Site 5 (Fig. 3), classified as high severity (dNBR = 906), illustrate the total loss of litter-duff layers and vegetation.

In Situ Data

The Bandelier National Monument Fire Ecology program collected site data before the Las Conchas Fire in July, August, and September from 2005 to 2007. Post-fire vegetation surveys were conducted in July 2012 and 2013, 1 to 2 yr post-fire, following the methods outlined by Brown (1974). Each site consisted of

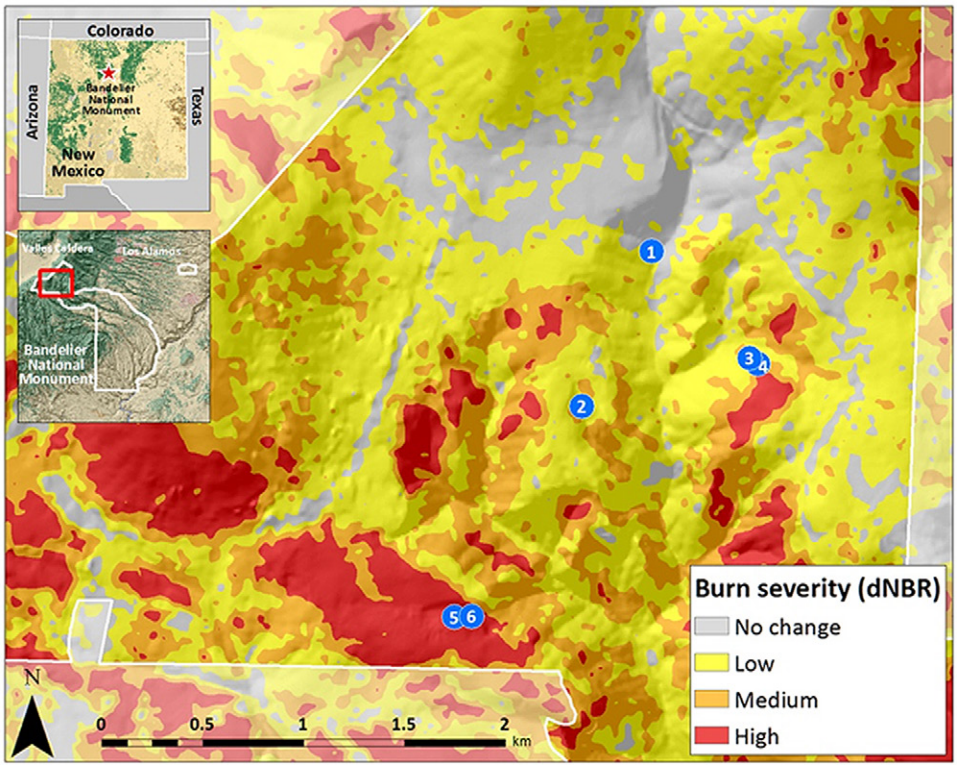

Fig. 2. Map of study area showing sites (1–6) in the upper Frijoles catchment. Burn severity is mapped using the relative differenced Normalized Burn Ratio (dNBR; Key and Benson, 2006) applied to the Rapid Assessment of Vegetation Conditions data set.

a 20- by 50-m (1000 m^2) area where all trees with a diameter at breast height (DBH) >15.0 cm were recorded and identified by species. All tree genus, species, DBH, and status (live or dead) were also recorded in a 20- by 25-m (500 m^2) subarea for any tree DBH ranging from 2.5 to 15.0 cm. Litter-duff depths were measured at 10 points along four 15-m fuel transects at each site, for a total of 40 data collection points. Bare ground and understory and canopy vegetation cover percentage from 166 sampling points on two 50-m point-line intercept vegetation transects for each site were estimated. Measurements of bare ground percentage and litter-duff layer thickness pre- and post-fire (Table 1) are within reported ranges for the Jemez Mountains (Martin and Moody, 2001).

Burn Severity and Vegetation Parameters

To incorporate the impact of burn severity on vegetation parameters, LAI values from the six sites were estimated using pre- and post-fire vegetation observations. Calculating LAI for each species per site involved multiplying the total foliage (F_T, kg) by the specific leaf area (SLA, m^2/kg), the stem density (ρ_{stem}) for each species (Laughlin et al., 2011), and the DBH class ($\rho_{stem,spp,DBH}$, trees/ha), and finally dividing by the plot area, A (ha/m^2):

$$LAI_{spp,DBH} = \frac{F_{T,spp,DBH} SLA_{spp} \rho_{stem,spp,DBH}}{A} \quad [1]$$

The value of F_T was provided from species-specific relationships between DBH and total biomass by Jenkins et al. (2004). The LAI calculated for the forest canopy (LAI_c) is then the sum of the LAI for all the live trees of each species and DBH class. The LAI for the understory (LAI_{us}) was assumed to be the same for the pre- and post-fire vegetation at 2.16 to represent seasonal grasses (Olson et al., 2000) and vegetation <2 m in height (Breuer et al., 2003; Whittaker and Niering, 1975) that either persisted under the undisturbed forest canopy, resprouted after the fire, or were not

Table 1. Estimated pre- and post-fire leaf area index (LAI) based on allometric functions, measured depth of litter-duff layer, and the parameterized depth of the litter-duff layer used in the model. Note the following classification for dNBR: high severity (dNBR > 640), moderate severity (315 < dNBR > 640), low severity (dNBR < 315), and unburned (dNBR < 70).

Site	dNBR	Estimated pre-fire LAI_{model}	Estimated post-fire LAI_{model}	Measured pre-fire litter-duff depth	Measured post-fire litter-duff depth	Measured pre-fire bare ground	Measured post-fire bare ground
				cm		%	
1	116	4.63	3.68	3.3	0.76	1.5	10.5
2	233	6.41	3.82	3.05	0.76	0.9	5.4
3	405	3.56	2.25	3.3	0.76	0.9	4.2
4	415	3.31	2.3	2.29	0.76	1.8	1.8
5	906	4.66	0.17	4.32	0.25	0.9	84.4
6	925	3.85	0.11	3.81	0	2.4	89.45

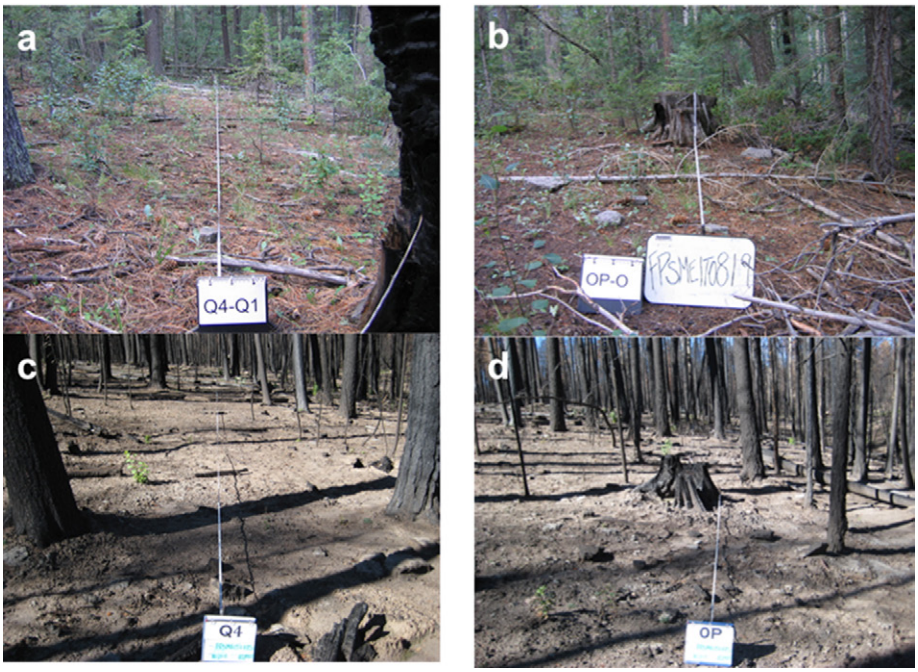

Fig. 3. Photographs taken (a,b) before and (c,d) after fire for a high severity burn, Site 5 (differenced normalized burn ratio = 906).

consumed by the fire. The weighted average between the canopy and understory LAI values and the measured bare ground cover percentage were used to assign the LAI:

$$\mathrm{LAI}_{\mathrm{model}} = \frac{\mathrm{LAI}_{\mathrm{c}}\left(1-\text{Bare soil \%}\right)}{2} + \frac{\mathrm{LAI}_{\mathrm{us}}\left(1-\text{Bare soil \%}\right)}{2} \quad [2]$$

Pre- and post-fire $\mathrm{LAI}_{\mathrm{model}}$ for each site (Table 1) are within the range of values from mixed conifer forest in northern New Mexico (Gower et al., 1992).

Burn Severity and Surface–Subsurface Parameterization

Post-fire simulations considered the changes in surface soil affected by burn severity by decreasing the saturated hydraulic conductivity in the top 2 cm of soil (K_{st}) as a function of dNBR, following Moody et al. (2016). The value of K_{st} was calculated for any dNBR >420:

$$K_{\mathrm{st}} = 390\exp\left(-0.0056\,\mathrm{dNBR}\right) \quad [3]$$

Moody et al. (2016) provided a relationship between burn severity and K_{st} based on measurements taken from the Palmer Divide, Colorado. Therefore, to provide an estimate of how K_{st} will change due to burn severity it was necessary to adjust the unitless coefficient to 390 to fit the assumed pre-fire hydraulic conductivity of the soils at our sites: 0.0325 m/h (Soil Survey Staff, 2015). Fire is documented to affect multiple infiltration parameters, including porosity and sorptivity, that generally reduce infiltration capacity but are not explicitly represented here, being assumed as captured by the lowering of the K_{st}, and noted as a longer term dominant soil hydrologic property change (Ebel et al., 2016). High severity burns were estimated to decrease K_{st} by more than an order of magnitude. Uncertainty in surface K_{st} due to burn severity was accounted for by simulating two standard deviations of the $\ln(K_{\mathrm{st}})$ (Table 2) based on Moody et al. (2016). The K_{st} uncertainty range was half an order of magnitude for each site, which accounts for moderate soil effects from low to moderate burn severity. Three post-fire simulations for each site were used to demonstrate post-fire K_{st} uncertainty in addition to the pre-fire simulation; this equated to 24 simulations for each year and 48 simulations in total.

Litter-duff layers are the measured dead plant material that either existed before the fire, were not consumed by the fire, or

Table 2. Differenced Normalized Burn Ratio (dNBR), parameterized pre- and post-fire surface soil (2-cm depth) saturated hydraulic conductivity (K_{st}), the estimated two standard deviations of $\ln(K_{\mathrm{s}})$ from Moody et al. (2016) (low and high K_{st}), and pre-and post-fire litter-duff depth.

Site	dNBR	Pre-fire K_{st}	Post-Fire K_{st}	Low K_{st}	High K_{st}	Pre-fire litter-duff depth	Post-fire litter-duff depth
		m/h				cm	
1	116	0.0325	0.0325	0.0179	0.059	3	1
2	233	0.0325	0.0325	0.0179	0.059	3	1
3	405	0.0325	0.0325	0.0181	0.0582	3	1
4	415	0.0325	0.0325	0.0181	0.0582	2	1
5	906	0.0325	0.00244	0.00134	0.0044	4	0
6	925	0.0325	0.00219	0.0012	0.004	4	0

accumulated since the fire and therefore are assumed to have the same hydraulic properties. They are explicitly represented in the model discretization as shown in Fig. 1 (Table 2) at 1-cm increments corresponding to the measured values in Table 1. The litter-duff layers were assigned van Genuchten parameters within the range of low bulk density and organic-C-rich forest soils (Teepe et al., 2003) (Table 3) and higher hydraulic conductivity and porosity than the underlying soil similar to Raaflaub and Valeo (2009). Mannings *n* (Table 3) was determined by the presence of a litter-duff layer or bare soil and assigned standard values from Dingman (2015).

Natural Resources Conservation Service soils data and existing literature on forest soils were used to estimate subsurface hydrologic parameters. Saturated hydraulic conductivity ranged from 0.015 to 0.05 m/h (Soil Survey Staff 2015) for soils in the upper Frijoles Canyon, simulated at 0.0325 m/h. The sandy loam porosity was approximated at 0.43 cm^3/cm^3 (Saxton et al., 1986). The van Genuchten parameters for soil were 1.43 and 19 (1/m) for *n* and α, respectively, and were representative of sandy loam (Ghanbarian-Alavijeh et al., 2010). The residual saturation of the soil was 0.05, characteristic of sandy loam (Rawls et al., 1982).

Spin-Up and Boundary Conditions

The model was spun up using measured precipitation, air temperature, wind speed, relative humidity, and incoming longwave and shortwave radiation data spanning 1 Jan. 2010 to 30 June 2013 from the headquarters meteorological station at the Valles Caldera National Preserve (Western Regional Climate Center, 2015), approximately 13 km from the sites. The spin-up set subsurface soil moisture conditions to an internally consistent variably saturated state (Maxwell, 2010) that determined antecedent soil moisture conditions before the forward simulation. The pre- and post-fire forward model used the same time series as a control for climate variability at a 10-min time step from 1 July to 31 August for the years of 2013 and 2014 (Fig. 4), thus resolving the hydrologic response to convective storm regimes (Moody et al., 2013; Spigel and Robichaud, 2007). Full meteorological inputs are shown in Supplemental Material SI.3. Precipitation in Bandelier is defined by a summer convective storm regime (Bowen, 1990) with intense initial rain pulses, where 80% of the total precipitation falls in the first 30 min. These seasonal storms between July and September make up to 40 to 70% of the total annual precipitation (Western Regional Climate Center, 2015).

Table 3. Domain hydrologic parameters.

Parameter	Soil	Litter-duff
Saturated hydraulic conductivity, m/h	0.0325	0.325
Mannings *n*, $h/m^{1/3}$	3×10^{-5}	5.8×10^{-5}
Porosity	43	65
Residual saturation	0.05	0.035
van Genuchten *n*	1.43	1.7
van Genuchten α, 1/m	19	10

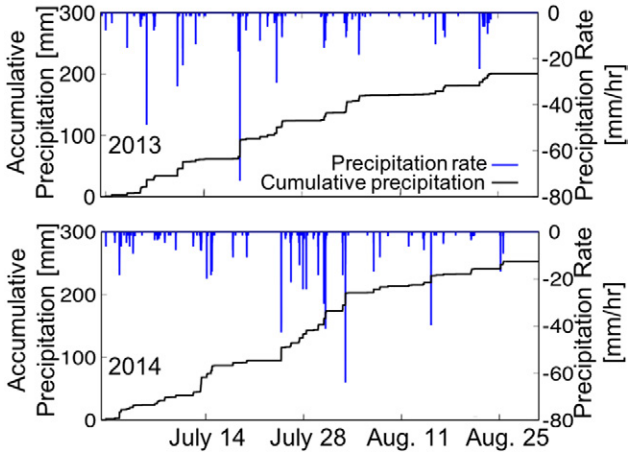

Fig. 4. Precipitation rate and cumulative precipitation for the simulated period between 1 July and 31 Aug. 2013 and 2014.

Results

Change in Hillslope Water Balance

Fire disturbance increased water storage for most sites by the end of the simulation, with the exception of the high burn severity sites. Figure 5 shows the final change in water storage (gray bars) between post-fire and pre-fire simulations and the changes in ET (blue bars) and runoff (red bars) that contributed to the final change in the water budget. It is important to note that the final change in the water budget is dependent on both the unique meteorological time series forcing the simulation and the arbitrary length of the simulation, as evident in the differences between the 2013 and 2014 water budget results. Nevertheless, important water budget responses to burn severity emerge from both simulation periods. Chiefly, the post-fire increase in water storage is highest in the low to moderate burn severity, and high burn severity surpasses a threshold that may result in a post-fire decrease in water storage. For the low to moderate burn severity simulations, the reduction of ET and therefore increase in soil water storage outweighed the enhanced runoff, resulting in increased soil water by the end of the simulation period. However, the high burn severity sites, specifically Site 6, crossed the zero threshold (Fig. 5), demonstrating that the post-fire conditions for high burn severity include potentially less soil water than pre-fire conditions.

The varying effects of burn severity on the overall amount of change in soil water storage follow similar trends for both years. Site 6 (highest burn severity) had a decrease in soil water storage for 2014 of 2% and the lowest increase in soil water storage in 2013 of only a 7% increase. Conversely, Site 1 (lowest burn severity) had the second smallest final change in soil water storage of 8% for 2013 and the lowest increase in soil water storage for 2014 of 7%. Furthermore, Site 2 (low burn severity) had the highest

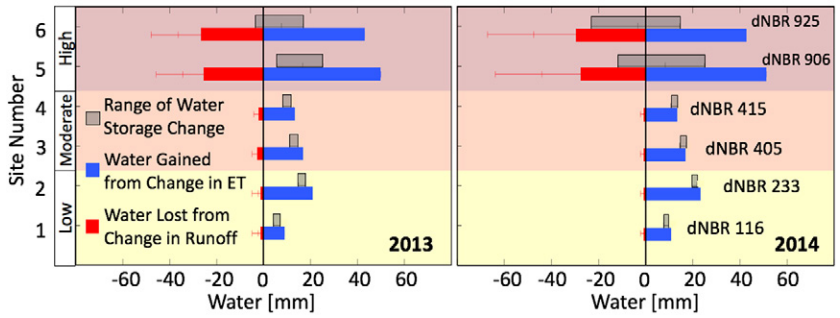

Fig. 5. The final difference between post-fire and pre-fire simulated water storage (post-fire minus pre-fire) for the 2013 and 2014 convective storm seasons (gray bars), the increase in water on the hillslope that is attributed to the change in evapotranspiration (ET) (pre-fire minus post-fire, blue bars), and the decrease in water on the hillslope that is associated with the increase in runoff (pre-fire minus post-fire, red bars). The decrease in water volume due to runoff also shows the uncertainty of runoff (error bars), which is due to the uncertainty of the surface soil saturated hydraulic conductivity (K_{st}) as a result of burn severity (Moody et al., 2016). The difference Normalized Burn Ratio (dNBR) is also shown for each of the six sites.

change in soil water storage, with a gain of 24% in 2013 and 32% in 2014. Sites 3 and 4 (moderate severities) had moderate changes in soil moisture for both simulation years. The variance in soil water storage as a function of burn severity suggests that the water balance components respond independently, where runoff increases nonlinearly with burn severity and ET reduces more linearly with increases in burn severity.

The transient comparison of the change in water storage (Fig. 6) demonstrates the time-dependent effect of each change to the water balance between components. Vertical drops in the change in water storage indicate runoff events, where prominent and frequent drops in water storage (Fig. 6) cumulatively produce larger water loss from changes in runoff (red bars; Fig. 5). Conversely, the steady increase in water storage with time is a result of the post-fire decrease in ET. The magnitude of the pre- and post-fire ET difference governs the slope of the change in water storage shown in Fig. 6. Steeper slopes for the change in soil water shown in the subplots of Fig. 6 result in a substantial water gain from ET (larger blue bars; Fig. 5).

The ascribed change in LAI drives the simulated response of decreased ET by transpiration reduction, which resulted in increased soil moisture for post-fire simulations. The change in total ET and all the components of ET—soil evaporation, transpiration, and interception—are shown in Fig. 7 and were consistent between the 2013 and 2014 seasons. Transpiration and interception decreased for all post-fire simulations, while evaporation from the soil surface increased. The overall decrease in total ET was due to the 13 to 95% decrease in transpiration, which is linearly dependent on LAI and the specific humidity difference between the evaporative surface and the atmosphere (Eq. [6] in Supplemental Material SI.2). Changes in LAI have only a tertiary effect on soil evaporation through increased soil temperature and the resulting specific humidity gradient (Eq. [4] in Supplemental Material SI.2).

The burn severity metric used in this study, dNBR, was shown to be related to changes in LAI (Boer et al., 2008); correspondingly ET changes in this study closely followed those of dNBR. Severely burned Sites 5 and 6 had the largest change in ET (42 and 39% decrease, respectively) and low burn severity Site 1 had the smallest decrease in ET (8% decrease). Likewise, moderately burned Sites 3 and 4 had slight LAI changes and a low to moderate reduction in total ET (14–17%). For comparison, using remote sensing products and the Operational Simplified Surface Energy Balance Model, Poon and Kinoshita (2018) observed a 20 to 36% reduction between pre- and post-fire ET for severely burned areas in the Las Conchas Fire, a 15 to 34% reduction for moderate burn severity, and 8 to 29% reduction for low severity. Interestingly, Site 2, with the second lowest burn severity (dNBR = 233), had the third highest estimated change in LAI (Table 1) and therefore showed a moderately strong decrease in ET. The combination of low dNBR (no K_{st} change), a slight increase in domain surface discharge, and a significant decrease in LAI is responsible for the large post-fire water storage increase in Site 2.

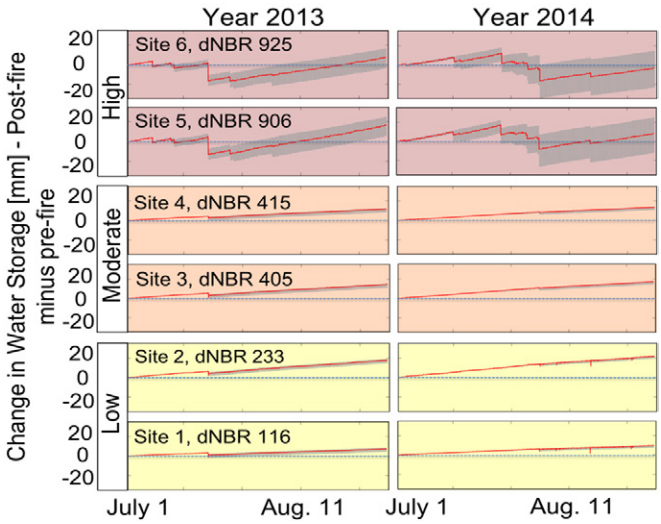

Fig. 6. Change in water storage time series showing the transient difference between post-fire and pre-fire simulations for each site. Plots compare the change in total water storage in the subsurface between post-fire simulations minus pre-fire simulations. The shaded gray areas in the subplots encapsulate the uncertainty due to changes in hydraulic conductivity [two standard deviations of $\ln(K_{st})$ of the top 2 cm of soil from the fire disturbance]. The sites for both plots are organized into low, moderate, and high burn severity categories, with specific differenced Normalized Burn Ratio (dNBR) values shown.

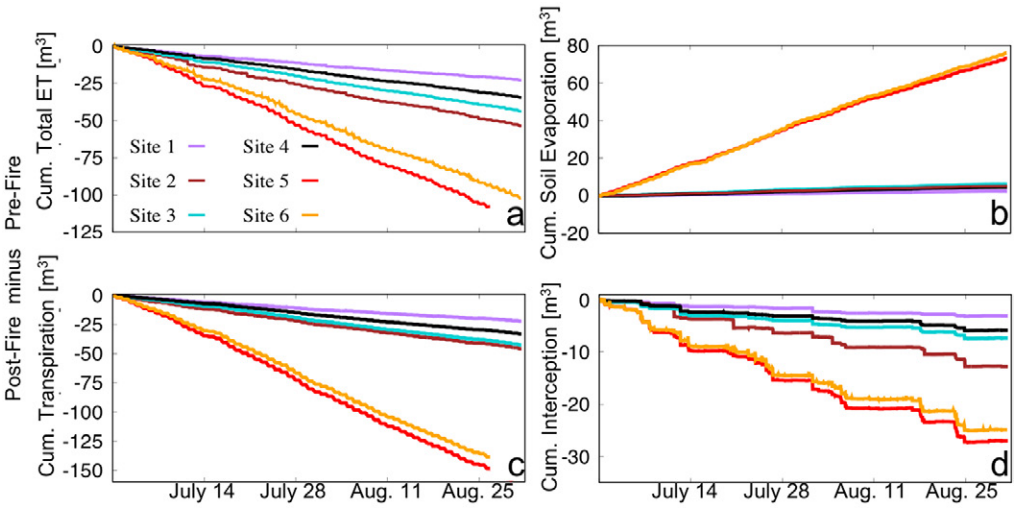

Fig. 7. The difference between cumulative pre-fire and post-fire evapotranspiration (ET) components: (a) total ET, (b) surface evaporation, (c) transpiration, and (d) canopy interception for the simulated monsoon season of 2013.

The amount of overland flow varied between each simulation but was largely a function of burn severity and the change in K_{st}, demonstrated by Sites 5 and 6 (high burn severity) and the respective high runoff (Fig. 5). Post-fire surface runoff to precipitation ratios ranged from 0.005 to 0.40 for the entire simulation period, with the highest simulated runoff depth of 67 mm, which when converted to volume of discharge from the domain is 168 m^3 from Site 6 (high-burn severity, 2014) as a result of having the lowest K_{st}. Severely burned Sites 5 and 6 had the most surface runoff and more instances of overland flow, indicated by multiple drops in the change in soil moisture (Fig. 6). In the high severity sites, the K_{st} uncertainty was propagated into the subsurface water storage (Fig. 6) only after overland flow events. Runoff also occurred on sites with no reduction in K_{st} at lower frequencies and magnitude, such as Site 2 (low-burn severity), which produced 1.02 mm in 2013. The runoff from the low severity sites was a result of the reduction of the litter-duff layer, which infiltrated and stored more water than the underlying soil.

The maximum hourly rainfall intensity or threshold intensity I_h^{thresh} (Moody and Martin, 2001) needed to produced infiltration-excess overland flow for Sites 5 and 6 was 9 mm/h. Nine storm events exceeded the I_h^{thresh} at the high burn severity sites in 2013 and 10 in 2014. The moderate and low burn severity sites did not initiate overland flow until an I_h^{thresh} of 48 mm/h; only two precipitation events in 2013 and one in 2014 exceeded an I_{30} of 48 mm/h. As I_{30} increases above the I_h^{thresh}, there is greater surface runoff magnitude (Moody and Martin, 2001).

The higher propensity of overland flow and strength of storms above the I_h^{thresh} in the severely burned sites resulted in a reoccurring loss of water and subsequently long periods of time when water storage in the post-fire simulations was less than pre-fire simulations. In fact, during the course of the 2013 and 2014 simulations, Sites 5 and 6 had less water storage for 33 to 55 and 50 to 77% of the time, respectively. An intense storm on 20 July 2013 demonstrated this shift in the water balance, when 40 and 50 m^3 of water for Sites 5 and 6, respectively, was discharged from the hillslope as surface runoff, amounting to 58 to 72%, respectively, of the precipitation from the storm. Nevertheless, the change in ET was also large for the severely burned sites, and the slopes of the change in the water storage plots were steeper.

Infiltration-Excess and Evapotranspiration

The competing effects of increased surface runoff and decreased ET with increased burn severity suggests an altered balance between the two processes. The total surface runoff difference between post-fire and pre-fire simulation is shown with the change in total ET (Fig. 8a and 8b) to illustrate the dominant effect on the water balance. A 1:1 correlation indicates no overall change in soil water storage. If surface runoff dominates the new water balance, then the site is drier and the data point is above the 1:1 line. Conversely, if ET dominates the post-fire water balance, then the site is wetter and the data point is below the 1:1 line. All sites were wetter with the exception of Site 6, and therefore the change in total ET dominated the water balance after fire disturbance. However, Site 6 had an increase in surface runoff that led to drier soil conditions. Site 6 and the lower band of K_{st} uncertainty for Site 5 demonstrate that severely burned sites with a significant decrease in infiltration capacity could increase overland flow and result in drier site conditions, especially for intense, convective storm events.

The loss of vegetation affected the site water balance over time by reducing the constant ET flux from the site. In contrast, overland flow was event based and occurred in short pulses. Cumulatively, the change in ET flux often dominated the new water balance. However, when compared with the episodic nature of overland flow and subsequent surface runoff events, a specific length of time was required at which the reduced ET flux from vegetation loss counterbalances the water lost from a given surface runoff event. Figure 8c illustrates the time needed for each site to match the water storage of the pre-fire conditions for a given volume of water lost to surface runoff. For example, runoff increases of 4 mm for Site 1 require 27 d of reduced ET to achieve

pre-fire soil moisture conditions; however, severely burned Sites 5 and 6 that had large reductions in ET required only 5 to 6 d of the reduced ET following 4 mm of additional surface runoff to achieve pre-fire soil moisture conditions. The increased runoff outweighs the decrease in ET for the severalty burned sites (Fig. 8a and 8b) even though the time needed to recover for a given amount of runoff is relatively short (Fig. 8c). This demonstrates the water balance tipping point induced by increased runoff and decreased infiltration capacity.

Discussion

Post-Fire Water Balance Changes

Many studies have documented both an increase in overland flow and soil moisture after fire disturbances (e.g., Ebel et al., 2016; Moody et al., 2008; Robichaud, 2000) when compared with other undisturbed locations. The numerical experiments presented in this study isolated the effects of burn severity and assessed whether a location becomes wetter or drier given the same meteorological forcing conditions. These numerical experiments confirmed previous observational studies (e.g., Cardenas and Kanarek, 2014; Ebel, 2013; Silva et al., 2006) and suggest that low to moderate fire disturbances will result in increased soil moisture due to decreased transpiration despite the increase in infiltration-excess overland flow. Moreover, by testing a gradation of burn severities, the simulations showed how net soil moisture could respond as burn severity increases. Site 1 (dNBR = 116) with the lowest burn severity showed small increases in soil moisture. Moderately burned Sites 3 (dNBR = 405) and 4 (dNBR = 415) resulted in moderate to high water storage gains. However, high severity burned Sites 5 (dNBR = 906) and 6 (dNBR = 925) had, in some cases, a water storage decrease in response to fire disturbance.

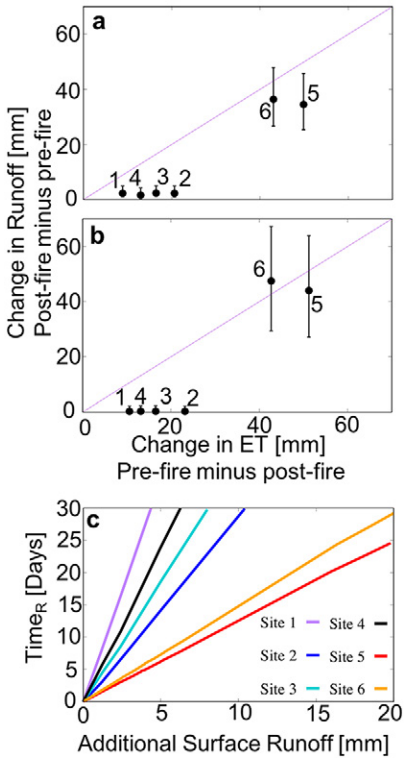

Fig. 8. The change in evapotranspiration (ET) vs. change in runoff for (a) 2013 and (b) 2014, and (c) the change in runoff vs. the amount of time needed for the decrease in ET to offset the water volume lost to runoff.

This work further demonstrated the dependency of soil moisture responses and the balance between infiltration-excess overland flow and transpiration, which may not always change proportionally as burn severity increases. Sites 2 and 6 demonstrated this dependency, where in cases of low burn severity (Site 2, dNBR = 233), the increase in surface runoff did not match the decrease in LAI. This is because the relationship between K_{st} and dNBR is nonlinear and at low burn severities the decrease in K_{st} is minimal whereas the decrease in LAI is linear with burn severity. The result is that Site 2 had one of the highest simulated increases in soil moisture. In the case of Site 6, the reduction in LAI, was small compared with the increase in surface runoff, resulting in a possible soil moisture decrease. This too is due to the nonlinear relationship between K_{st} and dNBR, reflecting a sharp decrease in K_{st} when dNBR is high.

Additionally, we identified a tipping point beyond which severely burned sites under heavy rainfall are drier as a result of increased surface runoff. During much of the post-fire simulations, severely burned Sites 5 and 6 had less soil moisture than the pre-fire simulations (Fig. 6), and the balance between the change in ET and the change in surface runoff shifted toward surface runoff domination. Only when enough time between intense precipitation events passed did the soil moisture in the post-fire simulations increase compared with the pre-fire simulations. This demonstrates that for a given window of time, the temporal distribution of storms that generate runoff will influence the measured change in the water budget.

The consequences of drier soil moisture conditions in severely burned areas include reduced groundwater recharge and site rehabilitation because seed germination requires suitable soil moisture conditions (Ayers, 1952; Fay and Schultz, 2009), especially in the near surface. Consistent with observational studies (Cardenas and Kanarek, 2014; Ebel, 2013), post-fire surface soils (top 1 cm) were drier than pre-fire surface soils during the time between precipitation events (Fig. 9). The loss of the litter and duff in combination with reduced LAI resulted in an increase in soil evaporation (Fig. 7b) (Villegas et al., 2010), which was primarily prevalent for Sites

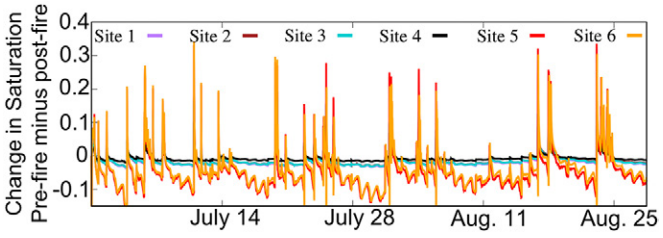

Fig. 9. The change in surface saturation in the top 1 cm of soil for post- and pre-fire simulations for simulation year 2013.

5 and 6 (severely burned). The reduced soil moisture from the increased surface runoff and the increase in surface soil evaporation has the potential to push the system into a new ecological regime, slowing forest regeneration or altering plant types (Pausas, 1999).

Dominant Processes and Burn Severity

The simulations in this study showed that the water balance change due to reduced transpiration often outweighed the water balance change due to increased runoff for low to moderate burn severity. A significant portion of the water balance is devoted to ET, which is >60% of the July and August precipitation for the pre-fire simulations. Nearby studies in lower elevation forests of the US Southwest document that 75 to 90% of June and July precipitation can be allocated to ET for unburned forests (Brandes and Wilcox, 2000). Given the significant portion of the water budget devoted to ET, changes to ET will produce substantial impacts to the water budget. However, as discussed above, the increased propensity for overland flow to occur in the severely burned sites due to a reduced K_{st} means that, at times, water lost to surface runoff will dominate the site water balance, which was generally the case for Sites 5 and 6. Moreover, the summer ET demand is high compared with other times of the year, such as winter, which would result in the steeper ET offset slopes depicted in Fig. 8c. Therefore, runoff generated when the ET demand is low such as winter or the snowmelt season will probably result in a longer site water deficit from the runoff event after fire disturbance. Likewise, the slightly lower reduction of ET for high severity sites documented by Poon and Kinoshita (2018) imply that the increased runoff may dominate the post-fire water balance more than reported in the current study, where a large decrease in LAI and therefore transpiration offsets the increase in surface runoff in the severely burned sites.

The balance between the change in overland flow and change in ET is also a function of precipitation intensity because discharge is governed by maximum rainfall intensity with similar burn severities (Moody et al., 2008). Reduced K_{st} by fire severity lowers the maximum rainfall intensity threshold, I_h^{thresh} (Moody and Martin, 2001), resulting in increased runoff. The precipitation time series of July and August from 2013 and 2014 sampled a range of rainfall intensities (Fig. 4), and the number of rainfall events varies year to year. If no precipitation events surpass I_h^{thresh}, then surface runoff will not occur and the change in ET will dominate the post-fire water balance. Conversely, increases in the magnitude and frequency of convective storms could move the system toward a surface runoff dominated regime. To predict how convective storm intensity (typical of southwestern regions with active fire regimes) will affect the hydrological response following fire disturbance, the new I^{thresh} needs to be qualified for a given burn severity. Based on this modeling experiment, if precipitation events and convective storm intensity increase, then the change in overland flow due to fire disturbance will probably dominate the post-fire water balance and soil moisture could decrease in response to fire disturbance.

Parameterizing Burn Severity into a Hydrologic Model

Translating burn severity metrics into meaningful hydrological parameters is imprecise, uncertain, and often requires extrapolations. For example, we used allometric relationships for measured tree species and DBH to parameterize LAI because direct measurements of LAI were unavailable. Extrapolating LAI from allometric relationships is not precise but rather an estimate using site-specific vegetation data. Furthermore, fire activity would probably damage the foliage in the surviving trees for post-fire LAI estimates. Therefore, it is likely that we overestimated post-fire LAI, and a higher change to ET and wetter site conditions may exist for the sites simulated here, with the notable exception of Sites 5 and 6. Severely burned Sites 5 and 6 had no measured living trees, and the only differences between the LAI (Table 1) was due to the observed bare ground percentage, which was used to estimate understory LAI (Eq. [2]). Therefore, it is likely that severely burned sites with a substantial reduction of infiltration capacity may be drier due to increases in surface runoff, given that LAI is as low as possible. Nevertheless, the first-order control of LAI on ET and the resulting site water balance demonstrates the importance of characterizing changes in LAI after fire disturbance. We therefore encourage monitoring programs to include reliable LAI measurements such as lidar surveys and forest densiometer measurements.

In addition to a reduction of LAI, fire disturbances have been found to reduce surface albedo (e.g., Veraverbeke et al., 2012) and change aerodynamic resistance terms such as surface roughness due to the canopy opening up (Chambers et al., 2005), which were not investigated here. While the overall change in local air temperature of burned ponderosa pine forests compared with unburned forest are minimal, notable increases to soil temperature and therefore soil evaporation may occur (Montes-Helu et al., 2009). Including burn severity effects to albedo and atmospheric mix terms may result in an additional increase in the soil evaporation and a smaller decrease in local ET. However, parameterization of albedo and atmospheric mix terms as a result of fire in US Southwest forests is not well constrained, and additional research is necessary to understand how these terms vary with burn severity.

Near-surface soil hydraulic conductivity is needed to simulate overland flow and soil moisture conditions. However, hydraulic conductivity is not typically monitored by land management surveys. Therefore K_{st} is highly uncertain due to variable fire behavior (Ebel et al., 2016). In this study, we parameterized the change in hydraulic conductivity using the relationship between dNBR and hydraulic conductivity as described by Moody et al. (2016). While we captured the uncertain change in K_{st} observed by Moody et al. (2016), the variation and heterogeneity of K_{st} is also large. Nonetheless, our simulations show that if K_{st} remains the same or increases, as is the case for the higher bounds of uncertainty for the low-severity sites, the overland flow may still increase due to reduced interception and the loss of the litter and duff layers. However, if we underestimated the decrease in K_{st}, then overland flow would increase, pushing sites to a surface runoff dominated regime. Additionally, spatial

heterogeneity of K_{st} as a result of fire disturbance would probably increase overall runoff but decrease the peak discharge (Ebel et al., 2016; Meyerhoff and Maxwell, 2011). As is the case with LAI, surface K_{st} is also considered a governing parameter and identified as a common soil response to burn severity in the literature (e.g., Martin and Moody, 2001; Moody et al., 2013; Robichaud, 2000). Therefore, characterizing K_{st} is necessary to represent the site water balance following fire disturbances. As a result, we encourage more studies such as Moody et al. (2016) to characterize the degree of soil change due to burn severity in multiple soil types.

Conclusion

As mega-fires are becoming prevalent, understanding the hydrologic response across a range of burn severities is increasingly necessary to quantify risks to water resources. In this work, ParFlow-CLM, a coupled surface and subsurface hydrologic model, was used to explore a range of burn severity parameters informed by data from the 2011 Las Conchas Fire. In situ data on vegetation, litter and duff depth, bare ground percentage, and burn severity was converted into surface and subsurface hydrologic parameters to isolate processes that govern hillslope water balance changes across seasonal timescales. Simulations showed that fire disturbances increased overland flow and soil moisture. The loss of vegetation and reduction of ET was found to dominate the water balance change. As burn severity increased, the competing hydrologic fluxes of ET and infiltration-excess overland flow offset each other. The significant change in ET was more dominant than water lost to overland flow at longer timescales. However, in cases of high burn severity, overland flow may dominate the site water balance, presenting a tipping point that leads to drier conditions. This work demonstrates how burn severity produces varied hydrological responses and specifically focused on previously undocumented processes of how competing effects of the change in ET and the change in runoff produce new hydrological regimes following fire disturbances.

Acknowledgments

The Los Alamos National Laboratory, Laboratory Directed Research and Development (LDRD), supported this work. We would like to acknowledge the hard work from the Bandelier National Monument Fire Ecology Field Team and Jennifer Paige. We further are indebted to two anonymous reviewers, whose valuable contributions and critique substantially improved the quality of this manuscript.

References

Ashby, S.F., and R.D. Falgout. 1996. A parallel multigrid preconditioned conjugate gradient algorithm for groundwater flow simulations. Nucl. Sci. Eng. 124:145–159. doi:10.13182/NSE96-A24230

Asner, G.P., J.M. Scurlock, and J.A. Hicke. 2003. Global synthesis of leaf area index observations: Implications for ecological and remote sensing studies. Global Ecol. Biogeogr. 12:191–205. doi:10.1046/j.1466-822X.2003.00026.x

Atchley, A.L., and R.M. Maxwell. 2011. Influences of subsurface heterogeneity and vegetation cover on soil moisture, surface temperature and evapotranspiration at hillslope scales. Hydrogeol. J. 19:289–305. doi:10.1007/s10040-010-0690-1

Ayers, A. 1952. Seed germination as affected by soil moisture and salinity. Agron. J. 44:82–84. doi:10.2134/agronj1952.00021962004400020006x

Bellot, J., A. Bonet, J. Sanchez, and E. Chirino. 2001. Likely effects of land use changes on the runoff and aquifer recharge in a semiarid landscape using a hydrological model. Landscape Urban Plann. 55:41–53. doi:10.1016/S0169-2046(01)00118-9

Bladon, K.D., M.B. Emelko, U. Silins, and M. Stone. 2014. Wildfire and the future of water supply. Environ. Sci. Technol. 48:8936–8943. doi:10.1021/es500130g

Boer, M.M., C. Macfarlane, J. Norris, R.J. Sadler, J. Wallace, and P.F. Grierson. 2008. Mapping burned areas and burn severity patterns in SW Australian eucalypt forest using remotely-sensed changes in leaf area index. Remote Sens. Environ. 112:4358–4369. doi:10.1016/j.rse.2008.08.005

Bowen, B.M. 1990. Los Alamos climatology. Lab Rep. LA-11735-MS. Los Alamos National Lab., Los Alamos, NM.

Brandes, D., and B.P. Wilcox. 2000. Evapotranspiration and soil moisture dynamics on a semiarid ponderosa pine hillslope. J. Am. Water Resour. Assoc. 36:965–974. doi:10.1111/j.1752-1688.2000.tb05702.x

Bréda, N., and A. Granier. 1996. Intra-and interannual variations of transpiration, leaf area index and radial growth of a sessile oak stand (*Quercus petraea*). Ann. For. Sci. 53:521-536. doi:10.1051/forest:19960232

Breuer, L., K. Eckhardt, and H.-G. Frede. 2003. Plant parameter values for models in temperate climates. Ecol. Modell. 169:237–293. doi:10.1016/S0304-3800(03)00274-6

Brown, J.K. 1974. Handbook for inventorying downed woody material. Gen. Tech. Rep. INT-16. US For. Serv., Intermtn. For. Range Exp. Stn., Ogden, UT.

Cannon, S.H. 2001. Debris-flow generation from recently burned watersheds. Environ. Eng. Geosci. 7:321–341. doi:10.2113/gseegeosci.7.4.321

Cannon, S.H., and S.L. Reneau. 2000. Conditions for generation of fire-related debris flows, Capulin Canyon, New Mexico. Earth Surf. Processes Landforms 25:1103–1121. doi:10.1002/1096-9837(200009)25:10<1103::AID-ESP120>3.0.CO;2-H

Cardenas, M.B., and M.R. Kanarek. 2014. Soil moisture variation and dynamics across a wildfire burn boundary in a loblolly pine (*Pinus taeda*) forest. J. Hydrol. 519:490–502. doi:10.1016/j.jhydrol.2014.07.016

Cawson, J., G. Sheridan, H. Smith, and P. Lane. 2012. Surface runoff and erosion after prescribed burning and the effect of different fire regimes in forests and shrublands: A review. Int. J. Wildland Fire 21:857–872. doi:10.1071/WF11160

Cawson, J., G. Sheridan, H. Smith, and P. Lane. 2013. Effects of fire severity and burn patchiness on hillslope-scale surface runoff, erosion and hydrologic connectivity in a prescribed burn. For. Ecol. Manage. 310:219–233. doi:10.1016/j.foreco.2013.08.016

Chambers, S.D., J. Beringer, J.T. Randerson, and F.S. Chapin. 2005. Fire effects on net radiation and energy partitioning: Contrasting responses of tundra and boreal forest ecosystems. J. Geophys. Res. 110:D09106. doi:10.1029/2004JD005299

Dahm, C.N., R.I. Candelaria-Ley, C.S. Reale, J.K. Reale, and D.J. Van Horn. 2015. Extreme water quality degradation following a catastrophic forest fire. Freshwater Biol. 60:2584–2599.

Dai, Y., X. Zeng, R.E. Dickinson, I. Baker, G.B. Bonan, M.G. Bosilovich, et al. 2003. The common land model. Bull. Am. Meteorol. Soc. 84:1013–1024. doi:10.1175/BAMS-84-8-1013

DeBano, L.F. 2000. The role of fire and soil heating on water repellency in wildland environments: A review. J. Hydrol. 231–232:195–206. doi:10.1016/S0022-1694(00)00194-3

Dingman, S.L. 2015. Physical hydrology. Waveland Press, Long Grove, IL.

Ebel, B.A. 2013. Simulated unsaturated flow processes after wildfire and interactions with slope aspect. Water Resour. Res. 49:8090–8107. doi:10.1002/2013WR014129

Ebel, B.A., F.K. Rengers, and G.E. Tucker. 2015. Aspect-dependent soil saturation and insight into debris-flow initiation during extreme rainfall in the Colorado Front Range. Geology 43:659–662. doi:10.1130/G36741.1

Ebel, B.A., F.K. Rengers, and G.E. Tucker. 2016. Observed and simulated hydrologic response for a first-order catchment during extreme rainfall 3 years after wildfire disturbance. Water Resour. Res. 52:9367–9389. doi:10.1002/2016WR019110

Fay, P.A., and M.J. Schultz. 2009. Germination, survival, and growth of grass and forb seedlings: Effects of soil moisture variability. Acta Oecol. 35:679–684. doi:10.1016/j.actao.2009.06.007

Ferguson, I.M., J.L. Jefferson, R.M. Maxwell, and S.J. Kollet. 2016. Effects of root water uptake formulation on simulated water and energy budgets at local and basin scales. Environ. Earth Sci. 75:316. doi:10.1007/s12665-015-5041-z

Ghanbarian-Alavijeh, B., A. Liaghat, G.-H. Huang, and M.Th. van Genuchten. 2010. Estimation of the van Genuchten soil water retention properties from soil textural data. Pedosphere 20:456–465. doi:10.1016/S1002-0160(10)60035-5

Gower, S.T., K.A. Vogt, and C.C. Grier. 1992. Carbon dynamics of Rocky Mountain Douglas-fir: Influence of water and nutrient availability. Ecol. Monogr. 62:43–65. doi:10.2307/2937170

Ice, G.G., D.G. Neary, and P.W. Adams. 2004. Effects of wildfire on soils and watershed processes. J. For. 102:16–20.

Jefferson, J.L., and R.M. Maxwell. 2015. Evaluation of simple to complex parameterizations of bare ground evaporation. J. Adv. Model. Earth Syst. 7:1075–1092. doi:10.1002/2014MS000398

Jefferson, J.L., R.M. Maxwell, and P.G. Constantine. 2017. Exploring the sensitivity of photosynthesis and stomatal resistance parameters in a land surface model. J. Hydrometeorol. 18:897–915. doi:10.1175/JHM-D-16-0053.1

Jenkins, J.C., D.C. Chojnacky, L.S. Heath, and R.A. Birdsey. 2004. Comprehensive database of diameter-based biomass regressions for North American tree species. Gen. Tech. Rep. NE-319. US For. Serv., Northeast., Res. Stn., Newtown Square, PA. doi:10.2737/NE-GTR-319

Jones, J.E., and C.S. Woodward. 2001. Newton–Krylov-multigrid solvers for large-scale, highly heterogeneous, variably saturated flow problems. Adv. Water Resour. 24:763–774. doi:10.1016/S0309-1708(00)00075-0

Kampf, S.K. 2011. Variability and persistence of hillslope initial conditions: A continuous perspective on subsurface flow response to rain events. J. Hydrol. 404:176–185. doi:10.1016/j.jhydrol.2011.04.028

Keeley, J.E. 2009. Fire intensity, fire severity and burn severity: A brief review and suggested usage. Int. J. Wildland Fire 18:116–126. doi:10.1071/WF07049

Key, C.H., and N.C. Benson. 2006. Landscape assessment (LA). In: D.C. Lutes et al., editors, FIREMON: Fire effects monitoring and inventory system. Gen. Tech. Rep. RMRS-GTR-164. US For. Serv., Rocky Mtn. Res. Stn., Fort Collins, CO. https://www.fs.fed.us/rm/pubs/rmrs_gtr164/rmrs_gtr164_13_land_assess.pdf

Kinoshita, A.M., A. Chin, G.L. Simon, C. Briles, T.S. Hogue, A.P. O'Dowd, et al. 2016. Wildfire, water, and society: Toward integrative research in the "Anthropocene". Anthropocene 16:16–27. doi:10.1016/j.ancene.2016.09.001

Kinoshita, A.M., and T.S. Hogue. 2011. Spatial and temporal controls on post-fire hydrologic recovery in Southern California watersheds. Catena 87:240–252. doi:10.1016/j.catena.2011.06.005

Kinoshita, A.M., and T.S. Hogue. 2015. Increased dry season water yield in burned watersheds in Southern California. Environ. Res. Lett. 10:014003. doi:10.1088/1748-9326/10/1/014003

Kollet, S.J., and R.M. Maxwell. 2006. Integrated surface–groundwater flow modeling: A free-surface overland flow boundary condition in a parallel groundwater flow model. Adv. Water Resour. 29:945–958. doi:10.1016/j.advwatres.2005.08.006

Kollet, S.J., and R.M. Maxwell. 2008. Capturing the influence of groundwater dynamics on land surface processes using an integrated, distributed watershed model. Water Resour. Res. 44:W02402. doi:10.1029/2007WR006004

Larsen, I.J., L.H. MacDonald, E. Brown, D. Rough, M.J. Welsh, J.H. Pietraszek, et al. 2009. Causes of post-fire runoff and erosion: Water repellency, cover, or soil sealing? Soil Sci. Soc. Am. J. 73:1393–1407. doi:10.2136/sssaj2007.0432

Laughlin, D.C., P.Z. Fule, D.W. Huffman, J. Crouse, and E. Laliberte. 2011. Climatic constraints on trait-based forest assembly. J. Ecol. 99:1489–1499. doi:10.1111/j.1365-2745.2011.01885.x

Littell, J.S., D.L. Peterson, K.L. Riley, Y. Liu, and C.H. Luce. 2016. A review of the relationships between drought and forest fire in the United States. Global Change Biol. 22:2353–2369. doi:10.1111/gcb.13275

Martin, D.A. 2016. At the nexus of fire, water and society. Philos. Trans. R. Soc. B 371:20150172. doi:10.1098/rstb.2015.0172

Martin, D.A., and J.A. Moody. 2001. Comparison of soil infiltration rates in burned and unburned mountainous watersheds. Hydrol. Processes 15:2893–2903. doi:10.1002/hyp.380

Maxwell, R.M. 2010. Infiltration in arid environments: Spatial patterns between subsurface heterogeneity and water–energy balances. Vadose Zone J. 9:970–983. doi:10.2136/vzj2010.0014

Maxwell, R.M. 2013. A terrain-following grid transform and preconditioner for parallel, large-scale, integrated hydrologic modeling. Adv. Water Resour. 53:109–117. doi:10.1016/j.advwatres.2012.10.001

Maxwell, R.M., and N.L. Miller. 2005. Development of a coupled land surface and groundwater model. J. Hydrometeorol. 6:233–247. doi:10.1175/JHM422.1

Merz, B., and E.J. Plate. 1997. An analysis of the effects of spatial variability of soil and soil moisture on runoff. Water Resour. Res. 33:2909–2922. doi:10.1029/97WR02204

Meyerhoff, S.B., and R.M. Maxwell. 2011. Quantifying the effects of subsurface heterogeneity on hillslope runoff using a stochastic approach. Hydrogeol. J. 19:1515–1530. doi:10.1007/s10040-011-0753-y

Mikkelson, K., R. Maxwell, I. Ferguson, J. Stednick, J. McCray, and J. Sharp. 2013. Mountain pine beetle infestation impacts: Modeling water and energy budgets at the hill-slope scale. Ecohydrology 6:64–72. doi:10.1002/eco.278

Montes-Helu, M.C., T. Kolb, S. Dore, B. Sullivan, S.C. Hart, G. Koch, and B.A. Hungate. 2009. Persistent effects of fire-induced vegetation change on energy partitioning and evapotranspiration in ponderosa pine forests. Agric. For. Meteorol. 149:491–500. doi:10.1016/j.agrformet.2008.09.011

Moody, J.A., and B.A. Ebel. 2012. Hyper-dry conditions provide new insights into the cause of extreme floods after wildfire. Catena 93:58–63. doi:10.1016/j.catena.2012.01.006

Moody, J.A., and B.A. Ebel. 2014. Infiltration and runoff generation processes in fire-affected soils. Hydrol. Processes 28:3432–3453. doi:10.1002/hyp.9857

Moody, J.A., B.A. Ebel, P. Nyman, D.A. Martin, C. Stoof, and R. McKinley. 2016. Relations between soil hydraulic properties and burn severity. Int. J. Wildland Fire 25:279–293. doi:10.1071/WF14062

Moody, J.A., and D.A. Martin. 2001. Post-fire, rainfall intensity–peak discharge relations for three mountainous watersheds in the western USA. Hydrol. Processes 15:2981–2993. doi:10.1002/hyp.386

Moody, J.A., D.A. Martin, S.L. Haire, and D.A. Kinner. 2008. Linking runoff response to burn severity after a wildfire. Hydrol. Processes 22:2063–2074. doi:10.1002/hyp.6806

Moody, J.A., R.A. Shakesby, P.R. Robichaud, S.H. Cannon, and D.A. Martin. 2013. Current research issues related to post-wildfire runoff and erosion processes. Earth Sci. Rev. 122:10–37. doi:10.1016/j.earscirev.2013.03.004

Olson, B., R. Wallander, and J. Beaver. 2000. Comparing nondestructive measures of forage structure and phytomass. Can. J. Plant Sci. 80:565–573. doi:10.4141/P99-073

Pausas, J.G. 1999. Response of plant functional types to changes in the fire regime in Mediterranean ecosystems: A simulation approach. J. Veg. Sci. 10:717–722. doi:10.2307/3237086

Pechony, O., and D.T. Shindell. 2010. Driving forces of global wildfires over the past millennium and the forthcoming century. Proc. Natl. Acad. Sci. 107:19167–19170. doi:10.1073/pnas.1003669107

Poon, P.K., and A.M. Kinoshita. 2018. Spatial and temporal evapotranspiration trends after wildfire in semi-arid landscapes. J. Hydrol. 559:71–83. doi:10.1016/j.jhydrol.2018.02.023

Raaflaub, L., and C. Valeo. 2009. Hydrological properties of duff. Water Resour. Res. 45:W05502. doi:10.1029/2008WR007396

Rawls, W., D. Brakensiek, and K. Saxton. 1982. Estimation of soil water properties. Trans. ASAE 25:1316–1320. doi:10.13031/2013.33720

Robichaud, P.R. 2000. Fire effects on infiltration rates after prescribed fire in Northern Rocky Mountain forests, USA. J. Hydrol. 231–232:220–229. doi:10.1016/S0022-1694(00)00196-7

Saxton, K., W.J. Rawls, J. Romberger, and R. Papendick. 1986. Estimating

generalized soil-water characteristics from texture. Soil Sci. Soc. Am. J. 50:1031–1036. doi:10.2136/sssaj1986.03615995005000040039x

Silva, J.S., F.C. Rego, and S. Mazzoleni. 2006. Soil water dynamics after fire in a Portuguese shrubland. Int. J. Wildland Fire 15:99–111. doi:10.1071/WF04057

Soil Survey Staff. 2015. Web soil survey. [Database.] Natl. Soil Surv. Lab., Lincoln, NE. http://websoilsurvey.nrcs.usda.gov (accessed 26 June 2015).

Soto, B., and F. Diaz-Fierros. 1997. Soil water balance as affected by throughfall in gorse (*Ulex europaeus*, L.) shrubland after burning. J. Hydrol. 195:218–231. doi:10.1016/S0022-1694(96)03232-5

Spigel, K.M., and P.R. Robichaud. 2007. First-year post-fire erosion rates in Bitterroot National Forest, Montana. Hydrol. Processes 21:998–1005. doi:10.1002/hyp.6295

Stoof, C.R., A.J. Ferreira, W. Mol, J. Van den Berg, A. De Kort, S. Drooger, et al. 2015. Soil surface changes increase runoff and erosion risk after a low–moderate severity fire. Geoderma 239–240:58–67. doi:10.1016/j.geoderma.2014.09.020

Teepe, R., H. Dilling, and F. Beese. 2003. Estimating water retention curves of forest soils from soil texture and bulk density. J. Plant Nutr. Soil Sci. 166:111–119. doi:10.1002/jpln.200390001

Tetzlaff, D., S.K. Carey, J.P. McNamara, H. Laudon, and C. Soulsby. 2017. The essential value of long-term experimental data for hydrology and water management. Water Resour. Res. 53:2598–2604. doi:10.1002/2017WR020838

Veraverbeke, S., W.W. Verstraeten, S. Lhermitte, R. Van De Kerchove, and R. Goossens. 2012. Assessment of post-fire changes in land surface temperature and surface albedo, and their relation with fire-burn severity using multitemporal MODIS imagery. Int. J. Wildland Fire 21:243–256 doi:10.1071/WF10075

Vertessy, R.A., R.G. Benyon, S.K. O'Sullivan, and P.R. Gribben. 1995. Relationships between stem diameter, sapwood area, leaf area and transpiration in a young mountain ash forest. Tree Physiol. 15:559–567. doi:10.1093/treephys/15.9.559

Villegas, J.C., D.D. Breshears, C.B. Zou, and D.J. Law. 2010. Ecohydrological controls of soil evaporation in deciduous drylands: How the hierarchical effects of litter, patch and vegetation mosaic cover interact with phenology and season. J. Arid Environ. 74:595–602. doi:10.1016/j.jaridenv.2009.09.028

Westerling, A.L., H.G. Hidalgo, D.R. Cayan, and T.W. Swetnam. 2006. Warming and earlier spring increase western US forest wildfire activity. Science 313:940–943. doi:10.1126/science.1128834

Western Regional Climate Center. 2015. Headquarters (VC) New Mexico. [Database.] Western Regional Clim. Ctr., Reno, NV. http://www.wrcc.dri.edu/cgi-bin/rawMAIN3.pl?nmvhvc (accessed 8 Oct. 2015).

Whittaker, R.H., and W.A. Niering. 1975. Vegetation of the Santa Catalina Mountains, Arizona: V. Biomass, production, and diversity along the elevation gradient. Ecology 56:771–790. doi:10.2307/1936291

Wine, M., and D. Cadol. 2016. Hydrologic effects of large southwestern USA wildfires significantly increase regional water supply: Fact or fiction? Environ. Res. Lett. 11:085006. doi:10.1088/1748-9326/11/8/085006

Woods, S.W., and V.N. Balfour. 2010. The effects of soil texture and ash thickness on the post-fire hydrological response from ash-covered soils. J. Hydrol. 393:274–286. doi:10.1016/j.jhydrol.2010.08.025

Wotton, B.M., C.A. Nock, and M.D. Flannigan. 2010. Forest fire occurrence and climate change in Canada. Int. J. Wildland Fire 19:253–271. doi:10.1071/WF09002